Soft Magnetic Composites Prepared by 3D Laser Printing

B. Kocsis[a,b,*], I. Fekete[a], I. Hatos[a] and L.K. Varga[b]

[a]Széchenyi István University Department of Materials Science and Technology,
1. Egyetem tér, Győr 9026, Hungary

[b]Wigner Research Center for Physics Inst. for Solid State Physics and Optics,
29-33 Konkoly-Thege út, Budapest 1121, Hungary

In this study, iron and inorganic insulator powders have been used for preparing soft magnetic metal-insulator type composites by 3D laser printing. These samples have been compared with those obtained by traditional pressing and sintering method. Considering the permeability spectra, an increase of the frequency limit has been found for the laser printed samples. In addition to the AC and DC magnetic parameters, the results of XRD and SEM investigations are also presented.

1. Introduction

The world's electricity consumption have set new records year after year since 2010. The latest record was in 2017 with 22016 TWh [1]. The continuous growth in energy demand, as shown in Fig. 1, with efficient and clean energy gratify provides proper driving forces for either the research, or the development of new and modern energy efficient materials.

Engineering magnetic materials (EMMs) play a prominent role in these developments. One of the most considerable subclasses of EMMs is soft magnetic materials (SMMs). The term "soft" refers to their coercive field, which is typically less than $H_c \leq 400$ A/m, high saturation of flux density, and high permeability which gives low energy consumption [2]. The most exemplary materials in this field are amorphous metals, nano-crystalline metals, silicon steel, ferrite, etc. These materials have two main loss types, hysteresis and eddy current losses. According to low coercive field, hysteresis loss can be kept to a minimum, but solution to reduce eddy current loss must also be taken into consideration. When a pure ferromagnetic material is well blended in an electrically insulating material, then the magnetic particles cannot produce such a large eddy current, so the resulting losses can be minimized. These materials are called soft magnetic composites (SMC). Many studies have already been carried out on the production of parts made of ferromagnetic powders mixed with polymer matrices [3, 4]. The problem is typically the inadequate adhesion of the matrix and ferromagnetic material resulting in the thermal and mechanical limitations. Low powder loading and inhomogenity is also a great limitation of these composites. Some scientific papers have already dealt with the issue of soft magnetic materials embedded in inorganic
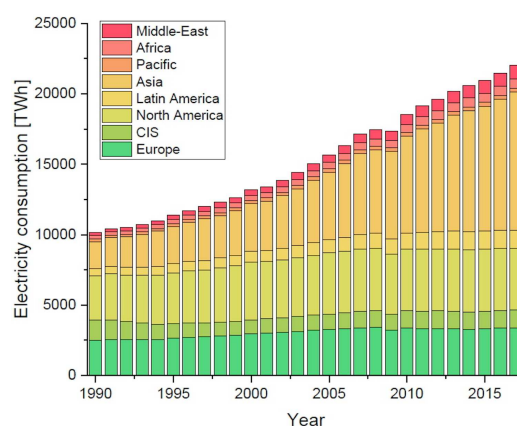

Fig. 1. World's electricity consumption from 1990 to 2017 [1].

insulating compounds [5]. In this study we have limited our experiments to this area. Samples were produced by an additive, the so-called direct metal laser sintering (DMLS) process. Then analyzed by various imaging techniques for their macro- and microstructure, also magnetic measurements were taken in order to characterise permeability spectra.

2. Experimental procedure

2.1. Phosphating treatment

The preparation of the printable SMC material consisted of iron powder and orthophosphoric acid diluted with isopropyl alcohol. The mixing ratios are given by A.H. Taghvaei et al. [5], the only modifications were the use of isopropyl alcohol instead of acetone. Phosphating treatment was carried out by stirring for 30 min while maintaining the mixing ratios. In one batch 250 grams of powder were prepared, which then was dried in a conditioning chamber at 40 °C and humidity 10%. Due to the volatile nature of isopropyl, it is suitable for degreasing of the iron powder and diluting the acid to the proper

———————

*corresponding author; e-mail: kocsis.bence@sze.hu

concentration. The orthophosphoric acid forms a simple iron-phosphate coating on the surface of the iron particles. The average size of powder particles was 100 μm and its purity was above 99.9% [5].

2.2. SMC fabrication

Two different powder technology methods were used to produce the samples. The first sample was prepared at elevated pressure and temperature, similarly to classic powder metallurgy sintering. At first, 40 grams of powder was loaded into a toroid-shaped sintering tool (ID = 10 mm; OD = 30 mm; Thickness = 9 mm). Then, it was precompressed and preheated at 350 °C for 30 minutes, and further compressed at 134 MPa on a conventional hydraulic press. The specimen was cooled down under pressure. In turn, the other specimens were produced by additive manufacturing on a EOSINT M270 laser sintering machine. The use of the DMLS method for this type of phosphated iron powder was innovative. Note that in the absence of any literature and manufacturer recommendations, we experimentally determined the near-ideal printing parameters.

2.3. Parameter optimization

Before starting the printing experiments, we defined 16 different programs (Table I) that we have used for printing $5 \times 5 \times 5$ mm^3. The first half of the samples (1–8) were scanned once with the laser, and the second half (9–16) was scanned twice.

Among the considered main parameters, the layer thickness (40 μm), the recoater speed (40 mm/s), the building platform temperature (100 °C) and the hatching strategy parameters were constant. The pre- and postcontours options that are responsible for pre- and postscanning of the contours were turned off in order to minimize the internal stresses in the pieces during the building process. This was necessary because the connection between the steel building platform and the molten iron-phosphate is not strong enough to resist high internal stresses. Accordingly, there were samples that detached from the building platform as the construction progressed. The printing process of these samples was terminated. In order to reduce internal stresses, we changed the hatch directions for samples scanned two times [6]. Finished specimen were inspected with computed tomography (CT) to determine the Fe–FePO$_4$-air ratio (Fig. 2).

CT scans were carried out with an YXLON Modular Y. CT system equipped with a 225 kV micro-focus X-ray tube and a Y.XRD1260 flat panel detector. CT scans of the samples were taken at a tube voltage of 190 kV acceleration voltage and 0.12 mA tube current. The flat panel detector was set to operate in a 2×2 binning mode with a 1000 ms integration time. There were taken 1440 projections without using filters. The resulting 1024^3 voxel data with a voxel size of 12.55 μm was loaded into VGStudio MAX for analysis. After the registration of the voxel dataset into a coordinate system, volume measurement of

Defined printing parameters.

TABLE I

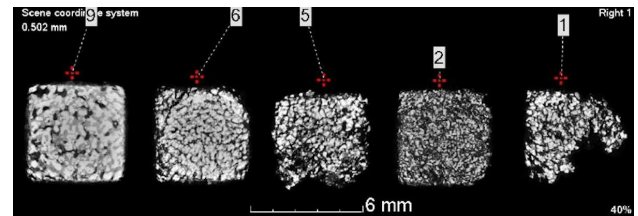| No.	$P_{1\,laser}$ [W]	v_1 [mm/s]	No.	$P_{1\,laser}$ [W]	v_1 [mm/s]	$P_{2\,laser}$ [W]	v_2 [mm/s]
1	10	100	9	10	100	10	100
2	10	200	10	10	100	12	100
3	10	300	11	10	100	15	100
4	10	400	12	10	100	20	100
5	15	100	13	20	100	10	100
6	20	100	14	20	300	10	100
7	25	100	15	20	500	10	100
8	30	100	16	20	800	10	100

Fig. 2. No. 1; 2; 5; 6; 9 cubic samples computed tomography images.

the components were done by analysing the histogram of the dataset. Volume measurement of porosity, iron and iron-phosphate was done by counting the voxels according to their density belonging to the appropriate material. The three types of material present in the samples resulted in three modes in the histogram, the valleys between the modes were used to identify threshold values. These threshold values separated the three materials in the histogram allowing for the summing of the values within these histogram ranges to get the volume of each material separately.

3. Results and discussion

Based on the CT measurements it is clear that as the specific energy input increases, the burning and the evaporation of the phosphate coating also increases. This results in a higher proportion of iron in the structure, and thus the Fe particles absorb more energy, Fig. 3.
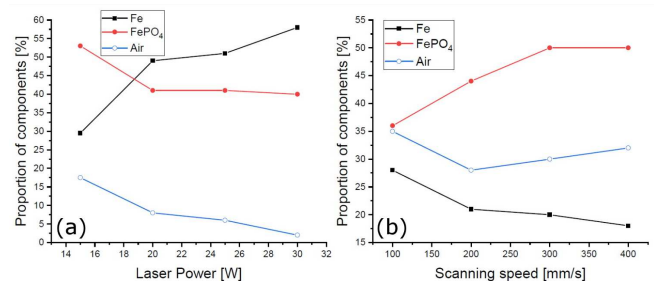

Fig. 3. The effect of laser power and scanning speed on the volumetric proportion of individual components.
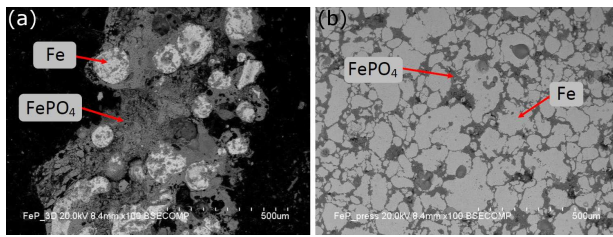
Fig. 4. 3D printed (a) and classic powder metallurgy sintering (b) samples scanning electron microscopic images.
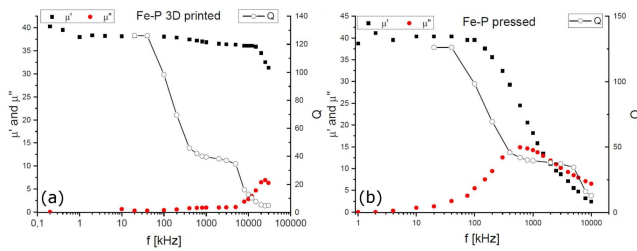

Fig. 5. (a) Permeability spectra for real (μ') and imaginary (μ'') components for exciting field amplitude. (b) Quality factor $Q = \mu'/\mu''$.
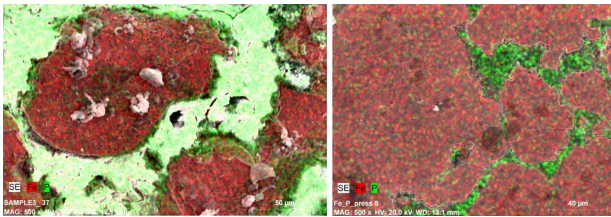

Fig. 6. 3D printed (left) and classic powder metallurgy sintering (right) samples scanning electron microscopic images.

The Fe powder melts partially or completely, leading to more compact structure. Note that the increased energy intake, after a certain level, damages the phosphate coating to such an extent that the electrically conductive portions are connected, and form a complete lattice structure. However, the coating is only partial. According to the scanning electron microscopy (SEM) measurements (Fig. 4), iron particles are denser in the pressed sample. In many cases, the individual Fe particles also come into contact with each other, or they may even fuse together.

With the additive manufacturing technology, we made samples of toroidal geometry (ID = 9 mm, OD = 30 mm, Thickness = 2 mm) for magnetic measurements. The imaginary and real permeability of the samples depending on the frequency of the excitation current was examined. The results are shown in Fig. 5.

Although the static permeability is similar for the two kinds of samples the high frequency behaviors are completely different. The frequency limit is shifted from

400 kHz for the pressed sample to 20 MHz (Fig. 5a) for the 3D laser printed sample. The electric percolation is more likely for the pressed sample involving the inter-particle eddy current whereas for printed sample the intra-particle eddy current prevails. The size of the particles as well as the thickness of the interlayer in the two cases is completely different. This is illustrated by SEM images taken with the same magnification in Fig. 6.

4. Conclusions

Our goal was to prove the possibility of additively manufacturing iron-phosphate SMC. The produced samples were electrically insulating, however mechanically weak. Experiences during manufacturing have shown that mechanical strength and electrical insulation cannot be performed simultaneously for this pair of materials. The sample prepared by classical sintering is more compact, more resistant to mechanical loads, but its electrical insulating capacity is not perfect. It may not be used effectively in the higher frequency range. The eddy current losses of the 3D printed sample start to increase only in the 10 MHz range, but its mechanical properties, density and homogeneity are far behind the other specimen. Since the printed sample was made with 10 W laser output at a scanning speed of 100 mm/s, which did not result in the most compact structure during the preliminary experiment. We are planning to produce toroidal samples with a higher laser performance. In the case of classical sintering, it may be worthwhile to try to produce sintered toroidal samples at different pressures and temperatures, in order to reduce the effect of percolation.

Acknowledgments

References

[1] Global Energy Statistical Yearbook, 2018.

[2] E. Périgo, B. Weidenfeller, P. Kollár, J. Füzer, Appl. Phys. Rev. 5, 031301 (2018).

[3] B. Khatri, K. Lappe, D. Nötzel, K. Pursche, T. Hanemann, Materials 11, 189 (2018).

[4] Y. Wang, F. Castles, P. Grant, Mater. Res. Soc. 1788, 29 (2015).

[5] A.H. Taghvaei, H. Shokrollahi, K. Janghorban, J. Alloys Compd. 481, 681 (2009).

[6] H. Ali, H. Ghadbeigi, K. Mumtaz, Mater. Sci. Eng. A 712, 175 (2017).